PERGAMON

International Journal of Heat and Mass Transfer 45 (2002) 4847–4856

International Journal of HEAT and MASS TRANSFER

www.elsevier.com/locate/ijhmt

Conductivity of granular media with stagnant interstitial fluids via thermal particle dynamics simulation

Watson L. Vargas, J.J. McCarthy *

Department of Chemical and Petroleum Engineering, University of Pittsburgh, Pittsburgh, PA 15261, USA

Received 23 July 2001; received in revised form 15 April 2002

Abstract

In this paper, a numerical technique—the thermal particle dynamics method (TPD)—is extended to study heat conduction in granular media in the presence of stagnant interstitial fluids. The method, which generates a multi-particle simulation by explicitly modeling many two-particle interactions, allows bed heterogeneities to be directly included and dynamic temperature distributions to be obtained at the particle-level. Comparison with experimental data shows that TPD yields quantitatively accurate values of the effective thermal conductivity without introducing new adjustable parameters for a wide range of stagnant interstitial media. The model not only sheds light on fundamental issues in heat conduction in particulate materials, but also provides a valuable test bed for existing continuous theories.

Keywords: Heat conduction; Granular material; Microstructure; Dynamic simulation

1. Introduction

Gaining understanding of heat transport in granular media from its microstructure is an old and important problem in many different fields, such as, powder processing, ceramics processing, powder metallurgy and packed bed reactor design. The formation and evolution of the microstructure within a particle packing is a dynamic process that involves a variety of different inter-particle forces (in addition to gravity) [1]. This microstructure, in turn, dictates the effective properties of the collective heterogeneous material (solid particles plus interstitial media) so that, ultimately, the individual particle properties play an important role in determining the bulk behavior of the system. In particular, the effective conductivity is strongly influenced by the contact mechanics exhibited by the particles—which may be elastic, plastic, elasto-plastic, visco-elastic, etc. [2].

Several theoretical and computational studies have been performed which examine the effects of contact deformation of smooth [3,4] and rough [2,5] elastic particles on the effective thermal conductivity, both explicitly accounting for the interstitial medium [2,6,7] as well as neglecting it (for example, assuming an interstitial vacuum) [4,8,9]. A discrete simulation technique for granular heat transfer, the thermal particle dynamics (TPD) method [10,11] has been shown to successfully predict the conductivity and transient temperature distribution of particle beds [10,11].

In this article the TPD technique is extended to incorporate the ability to model heat transport in particulate media in the presence of an interstitial fluid. While calculating transient temperature distributions is then possible, the focus here is on determining the effective conductivity (at steady state), for the sake of comparison with existing theories and experiments. In this context, the effective conductivity represents the ability of the system—particles plus fluid in the interstitial space—as a whole to transfer heat in response to an imposed gradient at the boundaries.

2. Thermal particle dynamics

The TPD simulation technique is based upon a traditional particle dynamics (PD) technique (often

* Corresponding author. Tel.: +1-412-624-7362; fax: +1-412-624-9639.

E-mail address: mccarthy@engrng.pitt.edu (J.J. McCarthy).

0017-9310/02/$ - see front matter
PII: S0017-9310(02)00175-8

Nomenclature

A	area (m^2)
a	contact radius (m)
ac	accomodation coefficient
c	specific heat ($J\,kg^{-1}\,K^{-1}$)
E^*	effective Young modulus (GPa)
F_n	normal force (N)
g	gravity ($9.8\ m\,s^{-2}$)
H	height in a 2-D bed (m)
H_c	contact conductance ($W\,m^{-2}\,K^{-1}$)
k	thermal conductivity ($W\,m^{-1}\,K^{-1}$)
ℓ	characteristic length (m)
P	pressure (Pa)
N	number of contacts
Q	heat transfer (W)
r	particle radius (m)
S	saturation
t	time (s)
T	temperature (K)
V	volume (m^3)
W	width in a 2-D bed (m)

Greek symbols

α	parameter in Eq. (21)
δ	parameter in Eq. (21)
ϵ	void fraction
ρ	density ($kg\,m^{-3}$)
v	Poisson ratio
ϕ	filling angle

Subscripts

c	contact
eff	effective
f	fluid
g	gas
i	particle i
j	particle j
l	liquid
s	solid
t	total

referred to as the discrete or distinct element method [12]) so that every particle is tracked individually to determine trajectories, velocities, forces and temperatures. This allows the determination of both mechanical and transport properties of granular systems under static or dynamic conditions. The particle trajectories are obtained via explicit solution of Newton's equations of motion for every particle [12]. The forces on the particles—aside from gravity—typically are determined from contact mechanics considerations [13].

The key feature of TPD is that by incorporating contact conductance theories many simultaneous two-body interactions may be used to model heat transfer in a system composed of many particles. In analogy with PD, this description requires that the time-step be chosen such that any disturbance (in this case a change in a particle's temperature) does not propagate further than that particle's immediate neighbors within one time-step. While for this work we are considering particles in lasting contact, this criterion is also satisfied in the majority of collision-dominated flows, although the amount of heat transferred between colliding particles under these conditions can be small [14].

2.1. General method

In terms of the conductance approach to heat transfer, the heat flow between the two particles (Fig. 1) is given by

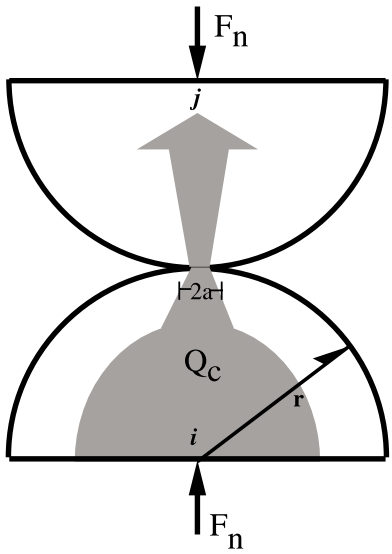

Fig. 1. Heat conduction between two smooth-elastic spheres.

$$Q_c = H_c\,\Delta T_{ij}, \tag{1}$$

where $\Delta T_{ij} = T_i - T_j$ is the temperature difference between the mid-planes of the spheres, and H_c is the contact conductance.

For smooth-elastic spheres in a vacuum, the contact conductance depends on the contact radius a which may be obtained from Hertz contact theory, so that the conductance may be expressed as

$$\frac{H_c}{k_s} = 2\left[\frac{3F_n r^*}{4E^*}\right]^{1/3} = 2a, \tag{2}$$

where E^* is the effective Young's modulus for the two particles, and r^* is the geometric mean of the particle radii. The evolution of the temperature of particle i (in some average sense) may then be given as

$$\frac{dT_i}{dt} = \frac{Q_i}{\rho_i c_i V_i}, \tag{3}$$

where T_i is the temperature of particle i, Q_i is the total amount of heat transported to particle i from its neighbor (particle j), and $\rho_i c_i V_i$ is the particle's "thermal capacity".

If the temperature gradients are confined to the region close to the contact spot, such that the ratio of the resistance inside the particle to the resistance between the particles as determine by the Biot number is small (i.e., $Bi = 2a/\pi r \ll 1$), then the individual heat flows between particles i and j (Q_{ij}) may be decoupled so that the total heat flow Q_i may be approximated as the sum of the interactions of particle i with each of it's neighbors, j, as

$$Q_i = \sum_{j=1}^{N} Q_{ij}. \tag{4}$$

The temperature of particle i, T_i, at time $t + \Delta t$ is calculated from

$$\begin{aligned} T_i^{t+\Delta t} &= T_i^t + \sum_{j=1}^{N} \Delta T_{ij}^{t+\Delta t} \\ &= T_i^t + \sum_{k=1}^{N} \left(T_j^t - T_i^t\right)\left(1 - \exp\left[-\frac{H_c}{\rho_i c_i V_i}\right]\Delta t\right). \end{aligned} \tag{5}$$

2.2. Interstitial fluids

The extension of TPD to include the effect of stagnant interstitial fluids (assumed to be explicitly applicable for small Rayleigh numbers; i.e., $Ra \ll 1.0$) is straightforward provided the following assumptions are met:

- the phases are assumed to be inert and thermally stable
- solid particles are non-porous
- the gas is insoluble in the liquid
- adsorption of the gas on the solid surface is negligible
- temperatures are continuous across all interfaces
- the conductivity of the interstitial fluid is small relative to that of the particle.

With these simplifications it is possible to assume that the total thermal conduction may be obtained from summing the contributions of each of the three mechanisms (all acting in parallel) considered here; (1) through the area of contact between particles, (2) through the gas phase, (3) and through the liquid phase. Also, that heat only flows between particles actually in contact since conduction through the interstitial fluids across larger gaps will be very slow. Therefore, the total contact conductance can be expressed as

$$H_t = H_c + H_g + H_l. \tag{6}$$

A general expression for the relative contributions of the fluid phase to the total conductance can be determined from the geometry of the system by

$$H_f = k_f\left[\frac{A_f}{\ell_f}\right], \tag{7}$$

where A_f is the area of contact—perpendicular to the heat flow—of the (individual) fluid phase and ℓ_f is a characteristic averaged length over which the flux applies. The problem then reduces to determining the areas of contact A_f of each of the respective interstitial fluid phases as well as calculating the corresponding averaged lengths ℓ_f in each of the cases considered. Once the total conductance is determined; H_c in Eq. (5) is replaced by H_t and the method of solution continues as described in Section 2.1.

Masamune and Smith [15], Kunii and Smith [16], Okazaki [17] and Yovanovich [7] have used similar reasoning to develop correlations for the effective conductivity of packed beds.

2.3. Interstitial gas

From the geometry of the system (see Fig. 2), H_g is calculated as follows: For a unit cell (two spheres in

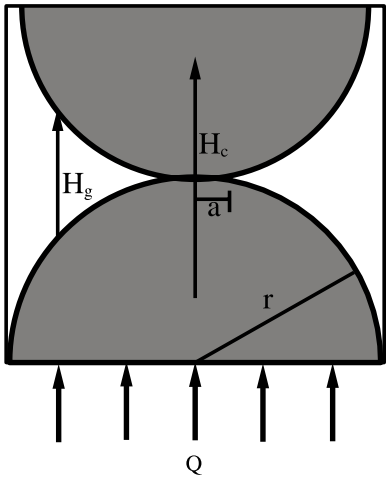

Fig. 2. Heat transfer model for particles in contact with a stagnant gas.

contact), the area exposed to the gas can be estimated as half of the particle's surface area minus the area of solid–solid contact and is given by

$$A_g = 2\pi r^2\left[1 - \frac{1}{2}\left(\frac{a}{r}\right)^2\right]. \tag{8}$$

The averaged length ℓ_g over which the heat flux applies can be determined as

$$\ell_g = \frac{r^2\left[1 - \frac{\pi}{4}\right]}{r - a}. \tag{9}$$

The conductance can then be expressed as

$$H_g = k_g^*\left[\frac{A_g}{\ell_g}\right] = k_g^*\left[\frac{2\pi\left[1 - \frac{1}{2}\left(\frac{a}{r}\right)^2\right](r-a)}{1 - \frac{\pi}{4}}\right], \tag{10}$$

where k_g^* is the gas conductivity appropriate for use over finite lengths (not necessarily large with respect to the mean free path of the gas molecules). This finite-length conductivity, k_g^*, has been related to the conductivity in an infinite gaseous medium, k_g, as a function of the interstitial gas pressure by Kennard [18]. Kennard's expression is developed for heat flow in the gas space between two parallel plates separated by a fixed distance [18], l, to yield

$$k_g^* = \frac{k_g}{\left[1 + \left(\frac{M}{l}\right)\right]}. \tag{11}$$

Following the approach of Masamune and Smith [15], we will use this expression for the conductivity between sphere surfaces by simply replacing l with our averaged length, ℓ_g (see Eq. (9)). The quantity M represents a length commonly referred to as the *temperature jump distance* [18] which can be estimated as

$$M = \left[\frac{2 - ac_1}{ac_1} + \frac{2 - ac_2}{ac_2}\right]\frac{\gamma}{\gamma + 1}\frac{1}{Pr}\Lambda, \tag{12}$$

where ac_1 and ac_2 are the thermal accommodation coefficients of the two surfaces and γ, Pr and Λ are the ratio of the specific heats, the Prandtl number, and the molecular mean free path, respectively. The mean free path Λ of the gas molecules is given by

$$\Lambda = \frac{k_B T}{\sqrt{2}\pi d_g^2 P}, \tag{13}$$

where P is the gas pressure, T is the temperature, d_g the diameter of the gas molecules and k_B is the Boltzman constant. It is important to note that the relations in Eqs. (11)–(13) introduce one empirical parameter, namely the accommodation coefficient ac. In keeping with the spirit of the TPD simulations, we do not use this constant as a freely adjustable parameter, instead we take it from results previously reported in the literature [18,19].

2.4. Interstitial liquid

Fig. 3 shows a unit cell for two particles in contact with a liquid bridge between them. Heat transfer is assumed to occur in one direction.

From the geometry of the system (see Fig. 3) the area for the liquid A_l, the gas A_g and the characteristic lengths ℓ_g and ℓ_l are determined as follows. If the filling angle ϕ for all particles in contact is approximately constant and fixed, and the particles are under a normal force (see Fig. 1), the interfacial surface area in contact with the liquid (modified from Rose [20]) is expressed as

$$A_l = 4\pi r^2\left[\left(\frac{\pi}{2} - \phi\right)\tan\phi - (1 - \cos\phi)\right] \times \left[\frac{1 - \cos\phi}{\cos\phi}\right] - \pi a^2. \tag{14}$$

The characteristic length ℓ_l for the heat flux through the liquid phase can be determined as

$$\ell_l = \frac{r_{cap}r - \left[\frac{r^2(\phi)}{2} + \frac{r_{cap}\sqrt{r^2 - r_{cap}^2}}{2}\right]}{r_{cap} - a}, \tag{15}$$

where r_{cap} is given as

$$r_{cap} = \sqrt{r^2(1 - \cos\phi)(1 + \cos\phi)}. \tag{16}$$

By a similar geometrical analysis, the surface area in contact with the gas, A_g, is the surface area of the particle minus the area for the liquid A_l and that of the solid–solid contact spot, so that

$$A_g = 2\pi r^2 - A_l - \pi a^2. \tag{17}$$

The characteristic length ℓ_g for the heat flux through the gas phase can be determined as

$$\ell_g = \frac{r^2\left[1 - \frac{\pi}{4}\right] - r_{cap}r - \left[\frac{r^2(\phi)}{2} + \frac{r_{cap}\sqrt{r^2 - r_{cap}^2}}{2}\right]}{r - r_{cap}}. \tag{18}$$

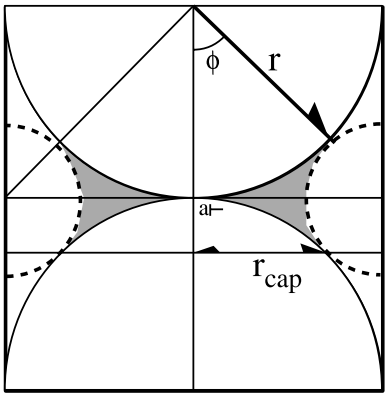

Fig. 3. Heat transfer model for particles in contact with a stagnant liquid.

3. Results and discussion

The emphasis in this work is on the development of a simulation technique to predict the effective thermal conductivity from first principles thus, we primarily treat particle beds composed of well characterized materials such as steel and glass in the presence of common gases and liquids. Unless otherwise stated, the solid properties used in this study are those of SS-304 and soda-lime glass (see Table 1).

For the two-dimensional (2-D) experiments the simulation consists of a mono-disperse system of perfectly smooth spheres forming a 2-D pseudo-regular packed bed (one particle deep) that has side lengths of roughly 30 particle diameters (to yield about 1100 particles). The particles are compressed at a known force either parallel or perpendicular to the direction of heating. All material properties are taken directly from the literature and consist solely of the thermophysical properties of the solids considered and the physico-chemical properties of the fluids. The bottom and top walls are kept at high and low temperature, respectively. Both the left and right walls are insulated. No effect of gravity is considered (i.e., the bed is assumed to be horizontal). It should be noted that there are no freely adjustable parameters in our simulation, however some of the correlations used in the estimation of fluid properties involved empirical parameters as described by the authors [21–24].

A typical initial condition for the 2-D simulations is obtained by perturbing a hexagonal lattice (by removing random particles from the lattice) and allowing the bed to resettle under an imposed load using a tradition isothermal PD simulation (particle mechanics only). The three-dimensional (3-D) beds tend not to form perfect crystalline structures and so no such measures are need for those simulations. The thermal conductivity for the various beds (2-D and 3-D) pressed at different loads with or without the presence of a fluid are determined using the steady-state values of the heat flows. This procedure mimics the most commonly used experimental techniques for the determination of effective thermal conductivity [25]. For 2-D (rectangular) beds, the effective conductivity is determined from

$$k_{\text{eff}} = -\frac{Q}{\left(\frac{Wd_{\text{p}}}{H}\right)\Delta T}, \tag{19}$$

where Q is obtained by summing the heat flows into/out of the particles in contact with the boundaries. It should be noted here that we ostensibly consider both low temperatures (on the order of 25 °C) and small temperature differences. In this way we may neglect radiation effects as well as variations in the solid phase conductivity. On the other hand, variation in the conductivity of the interstitial medium may be significant even at small temperature differences and these are not ignored (see Sections 3.1 and 3.2).

For the 3-D case a bed is created which mimics the well-known co-axial cylinder method and contains roughly 10,000 particles (being about 11 particles in radius and 25 long). The heat source here is represented by a core of radius R_1 comprised of particles which are maintained at a (high) constant temperature. The concentric cylindrical shell of radius R_2 that serves as heat sink is kept at a constant and lower temperature. The heat flow at equilibrium is then used to determine the effective conductivity of the bed as follows:

$$k_{\text{eff}} = -\frac{Q\ln(R_2/R_1)}{2\pi H\Delta T}. \tag{20}$$

Fig. 4 illustrates the setup as well as a snapshot of the temperature distribution at equilibrium for both the 2-D and 3-D computational experiments.

Table 1
Parameters used in the simulations

Parameter	SS-304	Soda-lime glass
Density ($\mathrm{kg\,m^{-3}}$)	7500	2600
Poisson ratio	0.29	0.25
Young's modulus (GPa)	193	70
Particle radius (m)	3.0×10^{-3}	3.0×10^{-3}
Thermal diffusivity ($\mathrm{m^2\,s^{-1}}$)	3.95×10^{-6}	5.1×10^{-7}
Thermal conductivity ($\mathrm{W\,m^{-1}\,K^{-1}}$)	15.0	1.1
Heat capacity ($\mathrm{J\,kg^{-1}\,K^{-1}}$)	506.0	800
Applied load (kg)	1.5–165	1.5–165
Friction coefficient	0.29	0.29

3.1. Gas–solid systems

The solids used in this part of the study are glass and SS-304 and the interstitial gases include air, CO_2 and helium. Beds ranging from 1000 to 10,000 particles have been used in the simulations with all the relevant thermal and physical properties taken from the literature. The accommodation coefficient ac in Eq. (12), is a function of both the gas and the solid surface properties. Based on the experimental data available [18,19], the following values for ac have been assumed: 0.95 for air, 1.0 for CO_2 and 0.3 for helium. Similar values have been used by Masamune and Smith [26], Zeng et al. [27] and Molerus [28].

3.1.1. Effect of gas pressure

Fig. 5 illustrates the effect of the interstitial gas pressure on thermal conductivity for a 2-D bed of steel particles at a constant load. The sharp increase with pressure is due to a transition from free-molecule conduction (when the mean-free path is large with respect to the mean separation) for which k_{g}^{*} is directly proportional to the pressure, to a regime dominated by

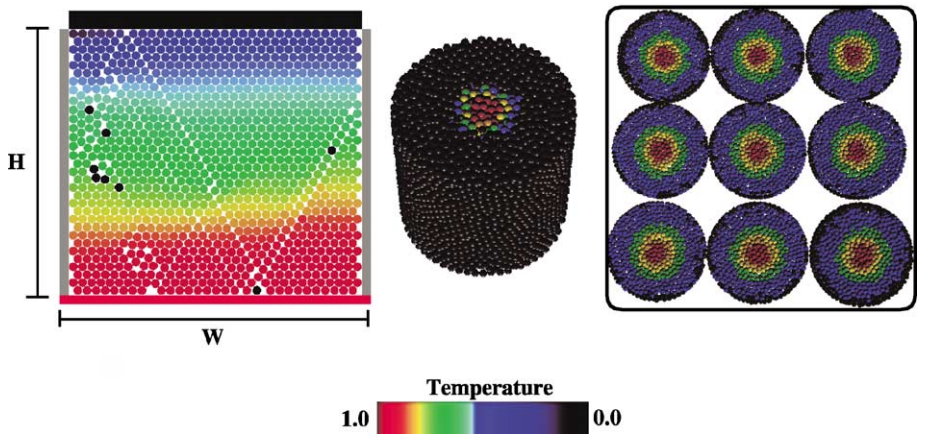

Fig. 4. Snapshot of the 2-D and 3-D computational setups for the determination of effective conductivity.

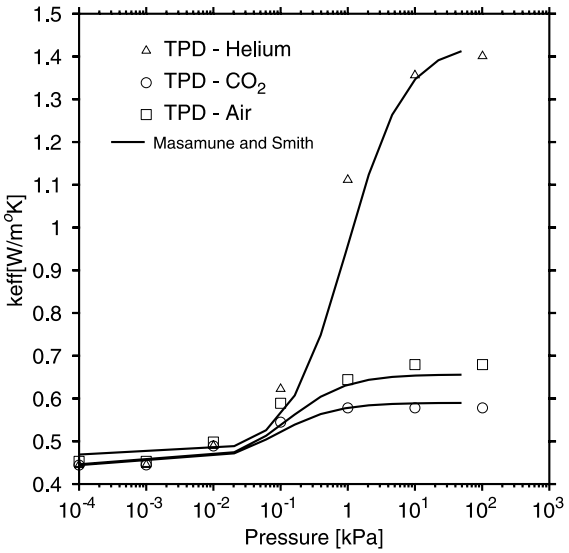

Fig. 5. Predicted thermal conductivity in a 2-D packed bed as a function of pressure of the filling gas. Symbols indicate TPD simulations, the continuous line the predictions based on Masamune and Smith [15] correlation.

molecular collisions in which k_g^* becomes independent of pressure and $k_g^* \simeq k_g$ (and the mean-free path is small compared with the mean separation) [26,29]. One should note that, under the conditions examine here (up to atmospheric pressure), the mean free path of Helium remains large compared to the mean particle separation. Experimental results qualitatively similar to those in Fig. 5 have been reported by Masamune and Smith [15,26], Bauer and Schlünder [19].

Masamune and Smith [15] have proposed a semi-empirical correlation for calculating the effective conductivity of packed beds in the presence of gases that incorporates essentially the same mechanisms considered in our TPD simulations. In terms of their notation the equation is written as

$$k_{\text{eff}} = \alpha\epsilon k_g + \frac{(1-\alpha\epsilon)(1-\delta)}{\frac{\phi}{k_g^*} + \frac{1-\phi}{k_g}} + (1-\alpha\epsilon)\delta k_s. \tag{21}$$

In Eq. (21) the terms on the right side represents the contribution of the (1) conduction in the void space, (2) a series path involving the solid and gas phases and, (3) conduction through the area of contact, respectively. The predictions based on this model are compared with those of a TPD simulation in Fig. 5. In Eq. (21) δ is regarded as a specific parameter for each type of particle and is related by an empirical expression (Eq. (15) in their paper) to the contact area, whose value is obtained by extrapolating the conductivity to zero pressure (vacuum conductivity). Using the extrapolated value at zero pressure as determined from the TPD simulations in calculating the δ parameter in Masamune's model it is possible to obtain a good quantitative agreement between the correlation and the data predicted by TPD as shown in Fig. 5.

3.1.2. Effect of external load

The effect of air pressure on particle beds compressed at three different loads is shown in Fig. 6. The results in Fig. 6 show that the external loading affects primarily the conductivity of the solid phase—the value of the effective conductivity extrapolated at zero pressure. It is expected that the significance of this difference will vary as the interparticle friction varies and stress chains within the materials become more or less stable (see Ref. [30]). All the profiles of effective conductivity reach a limiting value that is directly dependent on the effective conductivity at vacuum conditions. Note however that as the load increases the effect of loading on the solid phase conductivity also seem to reach a saturation

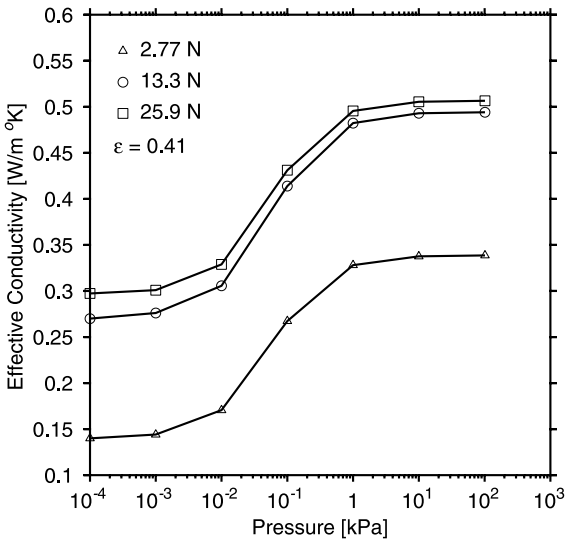

Fig. 6. Predicted thermal conductivity in a 3-D packed bed as a function of pressure of the filling gas highlighting the effect of external load. Note that the results are qualitatively similar to the 2-D curves in Fig. 5.

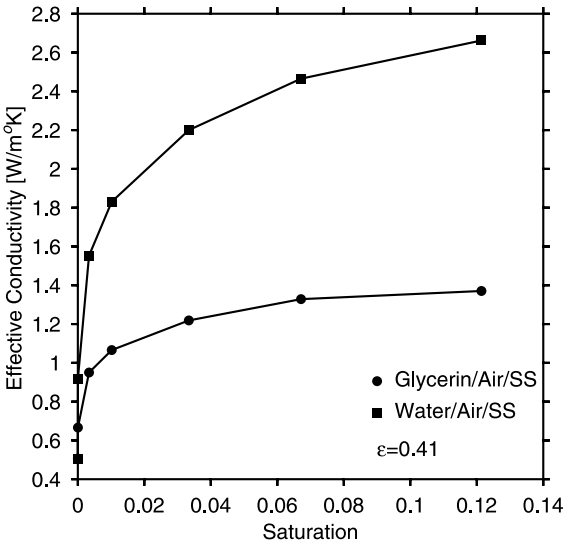

Fig. 7. Predicted thermal conductivity in a 3-D packed bed as a function of liquid saturation.

value—the separation of the curves at higher loads becomes smaller. A qualitative comparison with experimental data reported by Hadley [29] and Pratt [31] indicates that the shapes of the curves are similar.

3.2. Liquid–gas–solid systems

This set of numerical experiments are carried out with differing liquid bridge volumes of glass and SS-304 using water, glycerin and ethanol as interstitial fluids. Knowing both the volume of the liquid bridges and the number of contacts (bridges) per particle, the bed saturation is easily calculated. Furthermore, note that all the physico-chemical properties of the fluids as a function of temperature are taken from the literature [21,23].

3.2.1. Effect of saturation

Fig. 7 shows the variation of the effective thermal conductivity with fluid saturation. An increase of saturation degree up to about 10% results in a steep increase of the effective conductivity. Further increase of the saturation degree gives rise to higher values, however the rate of change is reduced. A simple interpretation for this observation can be made. Due to the fact that the resistance through the small solid contact spot is much higher than the one through the fluid cross-section, even a small liquid bridge can give rise to a steep increase in the effective conductivity, initially. In contrast, at higher saturations due to the curvature of the solid, an increase in the filling angle of the liquid bridge results in a small change in the cross section of the liquid bridge. Therefore, the increase of the effective conductivity becomes less pronounced at higher saturations. The predicted values in Fig. 7 are in reasonable agreement with the experimental observations provided by Okasaki [17] and Büssing and Bart [32].

3.2.2. Effect of external load

Fig. 8 illustrates the evolution of the effective thermal conductivity as a function of external load for a packed bed filled with spheres of SS-304 in the presence of air (at constant pressure) and water as the wetting fluid (at constant degree of saturation). As one might expect, the effect of an externally imposed load becomes less significant as the conductivity of the interstitial medium increases (i.e., from vacuum to gas to liquid).

Fig. 9 illustrates the relative contributions of the different mechanisms of heat transfer considered in this study, namely contact conductance, conduction through the gas phase and conduction through the liquid between particles, as a function of the external load. Note that, at low load and high saturation, the contribution of the heat flow due to contact conductance, Q_c, represents a relatively small percentage of the total heat transferred, but that this value increases significantly with either an increase in the level of external loading imposed or a decrease in the bed saturation. Moreover, the case examined in this figure represents a water/air/ss-304 system where the ratio of solid conductivity to liquid conductivity is relatively large. The effect of varying this ratio is explored in Section 3.2.3.

Fig. 9(b) shows that the contribution by contact conductance—in beds filled with only a stagnant gas—represents a significant fraction of the total heat when a

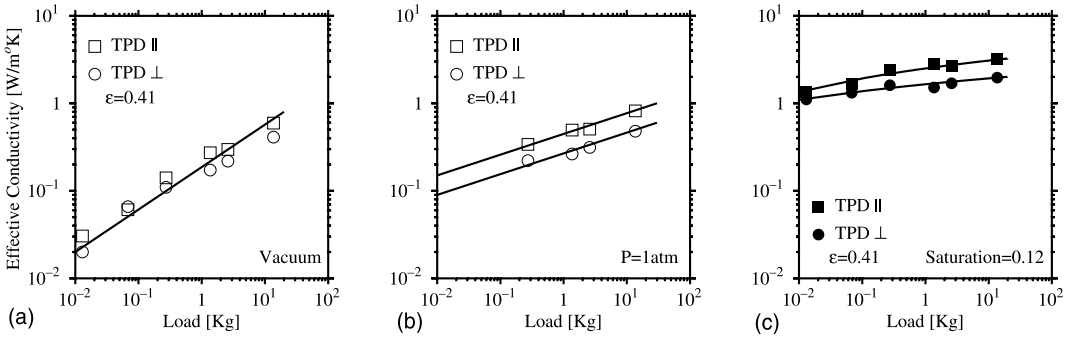

Fig. 8. Thermal conductivity in a 2-D packed bed as a function of load both parallel and perpendicular to the direction of the applied load. (a) Under vacuum, and in the presence of (b) gas (c) liquid plus gas.

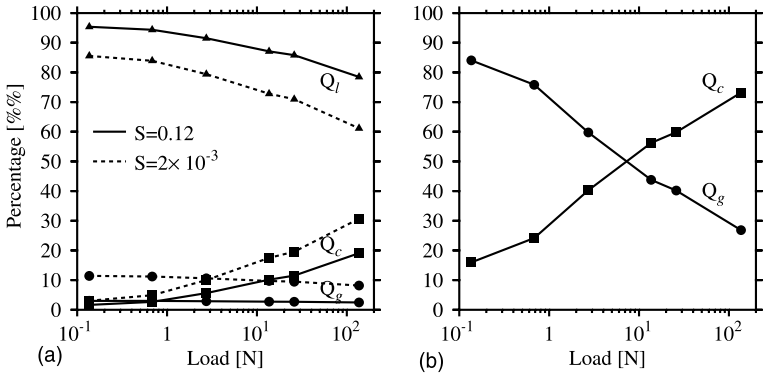

Fig. 9. Relative contributions of the heat transfer mechanisms in a 2-D packed bed to the overall heat transfer; (a) unsaturated bed (b) stagnant gas only.

moderate to high external load is imposed. Therefore, by changing the external load on a packed bed it is possible to alter the relative contributions of the different mechanisms involved and increase the effective conductivity (see Fig. 6).

3.2.3. Comparison with correlations and experimental data

A comparison between experimental values collected from literature and a typical correlation proposed by Hadley [29] is presented in Fig. 10.

The values predicted by TPD agree reasonably well both with experimental observations and with the semi-empirical correlation of Hadley. This suggests that the proposed method correctly reflects the effects of the mechanisms considered. It is worth mentioning that none of the experimental studies used for comparison explicitly report the load imposed on the samples used in their experimental measurements. The TPD simulated data used for comparison in Fig. 10 are based on predictions based on a 3-D packed bed with an external load of 10 kg. Therefore, we expect that this fact may

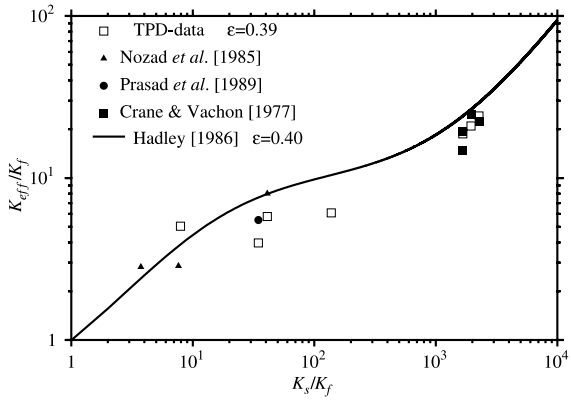

Fig. 10. Experimental and predicted values of the effective conductivity.

introduce some under or over-prediction since, as illustrated in Fig. 8, the effect of the external load on the effective thermal conductivity may be significant. In general, the values predicted from TPD seem to deviate

more from the experimental observations as the ratio k_s/k_f gets smaller. This behavior is not surprising since the model is built on the assumption that $k_s/k_f \gg 1$. As this ratio becomes smaller two effects become significant and cause the model to break down: heat transfer between non-contacting particles becomes comparable to that through the solid phase; the *Bi* is no longer small causing multi-particle heat transfer to become important and resulting in significant over-prediction of the conductivity by our model (see Fig. 10).

However, it is important to note the wide range of conductivities over which the model has been successfully applied, as well as the variety of fluids that have been used. Therefore, the present model can be used—within its limitations—to predict the results for a variety of measurements. The experimental data collected by Crane and Vachon [33], Prasad et al. [34] and Nozad et al. [35] has been used for comparison. Whenever possible the data used in the simulation corresponds closely with the data provided by the authors. For the diameter of the particles, a value of 3 mm was assumed when this variable was not specified.

4. Conclusions

The present work represents an attempt to treat both consolidated and unconsolidated beds of particles using first principles and a simple formalism. Note that some of the results mentioned here in the context of the heat transport problem have their analogues for other kind of transport problems (i.e., electric, mass transport), so that similar approaches may be applicable.

In this work, the TPD method—which provides both mechanical and thermal information about granular packings—has been extended to incorporate the effects of stagnant fluids. In particular, this technique is employed to simulate heat conduction in packed beds of particles and our results are compared to both experiments and theoretical predictions from the literature. Despite the simplicity of TPD and the idealized conditions used, good qualitative agreement for the predicted values of the effective thermal conductivity are obtained without requiring any freely adjustable parameters.

It has been demonstrated that for $k_s/k_f \gg 1$, TPD provides good qualitative and quantitative agreement between measured and calculated values of the effective conductivity for a wide variety of materials and for packed beds at different loads in the presence of both liquid and/or gases.

As presented in this work, the TPD method considers conduction through a bed of identical, elastic, smooth particles in the presence of stagnant interstitial fluids; however, this method is eminently extensible. Differing contact mechanics, and therefore contact conductance, can be easily included to assess the effect of particle roughness and/or plasticity. Including variations in particle mechanical and thermal properties as a function of temperature is also easily achieved. Perhaps more interesting, however, is the fact that, being built upon a granular flow simulation, TPD is useful for studying heat transfer in moving granular materials as well (where characterization of the changing microstructure is nearly impossible). The extension to incorporate fluid flow is currently under development.

Acknowledgements

The authors would like to acknowledge the support of the Central Research Development Fund of the University of Pittsburgh as well as the Dow Chemical Company for partial support of this research.

References

[1] L.F. Liu, Z.P. Zhang, A.B. Yu, Dynamic simulation of the centripetal packing of mono-sized spheres, Phys. A 268 (1999) 433–453.
[2] G. Buonanno, A. Carotenuto, The effective thermal conductivity of a porous medium with interconnected particles, Int. J. Heat Mass Transfer 40 (1997) 393–405.
[3] A.Z. Zinchenko, Effective conductivity of loaded granular materials by numerical simulation, Phil. Trans. R. Soc. Lond. A 356 (1998) 2953–2998.
[4] A.K.C. Wu, S.H.-K. Lee, Sphere packing algorithm for heat transfer studies, Numer. Heat Transfer, Part A 37 (2000) 637–651.
[5] G. Buonanno, A. Carotenuto, The effective thermal conductivity of packed bed of spheres for a finite contact area, Numer. Heat Transfer, Part A 37 (2000) 343–357.
[6] G.J. Cheng, A.B. Yu, P. Zulli, Evaluation of effective thermal conductivity from the structure of a packed bed, Chem. Eng. Sci. 54 (1999) 4199–4209.
[7] M.M. Yovanovich, Thermal contact resistance across elastically deformed spheres, J. Spacecraft Rockets 4 (1967) 119.
[8] C.K. Chan, C.L. Tien, Conductance of packed spheres in vacuum, J. Heat Transfer 95 (1973) 302–308.
[9] A.M. Clausing, B.T. Chao, Thermal contact resistance in a vacuum environment, J. Heat Transfer 87 (1965) 243–251.
[10] W.L. Vargas, J.J. McCarthy, Heat conduction in granular materials, AIChEJ 47 (2001) 1052–1059.
[11] W.L. Vargas, J.J. McCarthy, Stress effects on the conductivity of particulate beds. Chem. Eng. Sci., 57 (2002) 3119–3131.
[12] P.A. Cundall, O.D.L. Strack, A discrete numerical model for granular assemblies, Géotechnique 29 (1979) 47–65.
[13] K.L. Johnson, Contact Mechanics, Cambridge University Press, Cambridge, 1987.
[14] J. Sun, M.M. Chen, A theoretical analysis of heat transfer due to particle impacts, Int. J. Heat Mass Transfer 31 (1988) 969–975.

[15] S. Masamune, J.M. Smith, Thermal conductivity of beds of spherical particles, I&EC Fundamentals 2 (1963) 136–143.
[16] D. Kunii, J.M. Smith, Heat transfer characteristics of porous rocks, AIChEJ 6 (1960) 71–77.
[17] M. Okazaki, Heat and mass transport properties of heterogeneous materials, Drying'85 (1985) 84–96.
[18] E.H. Kennard, Kinetic Theory of Gases, McGraw-Hill, N.Y, 1938.
[19] R. Bauer, E.U. Schlünder, Effective radial thermal conductivity of packings in gas flow. Part II. Thermal conductivity of the packing fraction without gas flow, Int. Chem. Eng. 18 (1978) 189–204.
[20] W. Rose, Volumes and surface areas of pendular rings, J. Appl. Phys. 4 (1958) 687–691.
[21] R.C. Reid, J.M. Prausnitz, B.E. Poling, The Properties of Gases and Liquids, McGraw-Hill, N.Y, 1987.
[22] J.F. Shackelford, Introduction to Materials Science for Engineers, Macmillan, N.Y, 1985.
[23] N.B. Vargaftik, L.V. Filippov, A. Tarzimanov, E. Totskii, Handbook of Thermal Conductivity of Liquids and Gases, CRC Press, London, 1994.
[24] B. Le Neindre, R. Tufeu, P. Bury, P. Johannin, B. Vodar, The thermal conductivity coefficients of some noble gases, in: C.Y. Ho, R.E. Tylor (Eds.), Thermal Conductivity, Plenum Press, N.Y, 1969, pp. 75–100.
[25] A. Dutta, R.A. Mashelkar, Thermal conductivity of structured liquids, Adv. Heat Transfer 18 (1987) 161–239.
[26] S. Masamune, J.M. Smith, Thermal conductivity of porous catalyst pellets, J. Chem. Eng. Data 8 (1963) 54–58.
[27] S.Q. Zeng, A. Hunt, R. Greif, Mean free path and apparent thermal conductivity of a gas in a porous medium, J. Heat Transfer 117 (1995) 758–761.
[28] O. Molerus, Heat transfer in moving beds with a stagnant interstitial gas, Int. J. Heat Mass Transfer 40 (1997) 4151–4159.
[29] G.R. Hadley, Thermal conductivity of packed metal powders, Int. J. Heat Mass Transfer 29 (1986) 909–920.
[30] C. Thornton, S.J. Anthony, Quasi-static deformation of particulate media, Phil. Trans. R. Soc. Lond. A 356 (1998) 2763–2782.
[31] A.W. Pratt, Heat transmission in low conductivity materials, in: R.P. Tye (Ed.), Thermal Conductivity, Academic Press, London, 1969, pp. 312–313.
[32] W. Büssing, H.J. Bart, Thermal conductivity of unsaturated packed beds—comparison of experimental results and estimation methods, Chem. Eng. Process. 36 (1997) 119–132.
[33] R.A. Crane, R.I. Vachon, A prediction of bounds on the effective thermal conductivity of granular materials, Int. J. Heat Mass Transfer 2 (1977) 711–723.
[34] V. Prasad, N. Kladias, A. Bandyopadhaya, Q. Tian, Evaluation of correlations for stagnant thermal conductivity of liquid-saturated porous beds of spheres, Int. J. Heat Mass Transfer 32 (1989) 1793–1796.
[35] I. Nozad, R.G. Carbonell, S. Whitaker, Heat conduction in multiphase flows—II, Chem. Eng. Sci 40 (1985) 857–863.